

Dynamical Corrections to Spin Wave Excitations in Quantum Wells due to Coulomb Interactions and Magnetic Ions

Cynthia Aku-Leh,^{1,2} Florent Perez,¹ Bernard Jusserand,¹ David Richards,² and Grzegorz Karczewski³

¹*Institut des Nanosciences de Paris, UMR 7588, CNRS/Université Paris VI et VII, Campus Boucicaut, 140 rue de Lourmel, 75015 Paris, France*

²*Department of Physics, King's College London, Strand, London WC2R 2LS, United Kingdom*

³*Institute of Physics, Polish Academy of Sciences, al. Lotników 32/46, 02-668 Warszawa, Poland*

(Dated: April 24, 2022)

We have measured dispersions of spin-flip waves and spin-flip single-particle excitations of a spin polarized two-dimensional electron gas in a $\text{Cd}_{1-x}\text{Mn}_x\text{Te}$ quantum well using resonant Raman scattering. We find the energy of the spin-flip wave to be below the spin-flip single particle excitation continuum, a contradiction to the theory of spin waves in diluted magnetic semiconductors put forth in [Phys. Rev. B **70** 045205 (2004)]. We show that the inclusion of terms accounting for the Coulomb interaction between carriers in the spin wave propagator leads to an agreement with our experimental results. The dominant Coulomb contribution leads to an overall red shift of the mixed electron-Mn spin modes while the dynamical coupling between Mn ions results in a small blue shift. We provide a simulated model system which shows the reverse situation but at an extremely large magnetic field.

PACS numbers: 72.25.Dc, 73.21.-b, 78.30.-j, 78.55.-m

I. INTRODUCTION

Collective spin dynamics in dilute magnetic semiconductors (DMS) is an active field under intense investigations.¹⁻⁴ This field provides an insight into the origins of carrier-induced ferromagnetism in semiconductors⁴⁻⁹ and an understanding of particular features of the DMS^{6,10} due to the presence of two spin sub-systems that are dynamically coupled via Coulomb-exchange interaction: that of the itinerant carrier and that of the localized magnetic impurities. As an example of these features, the transverse spin excitation spectrum has been theoretically found to be composed of three types of excitations. These are: two collective excitations corresponding to itinerant and localized spins precessing in phase or out of phase to each other, and single-particle (or Stoner-like) excitations of the itinerant carriers.^{6,10,11} The in-phase collective mode is the Goldstone-like mode. The out of phase mode has a dominant contribution from the itinerant carrier subsystem.^{6,11} Experimental evidences of the entire spectrum in ferromagnetic DMS like GaMnAs is not available. Reported so far are features related to the zone-center in phase mode, dominated by the Mn spin precession, its dynamics^{3,12,13} and its ferromagnetic resonance.¹⁴ We find no experimental data available for the out of phase mode. Indeed, ferromagnetism in GaMnAs systems requires a high Mn concentration, which destroys the quality of the crystal potential and smooths out all optical resonances.

To gain more insight into the DMS spin excitation spectrum, $\text{Cd}_{1-x}\text{Mn}_x\text{Te}$ doped quantum wells are a very good alternative as they are clean and efficient to capture the general properties of the collective spin dynamics in DMS materials. The high quality of $\text{Cd}_{1-x}\text{Mn}_x\text{Te}$ quantum well structures leads to a high mobility of the itinerant gas (electrons or holes) together with well-defined

optical resonances,¹⁵ an important condition for the observation of electronic Raman signals from the carrier subsystem.¹⁶ The presence of Mn impurities interacting with the two dimensional electron gas (2DEG) embedded in the $\text{Cd}_{1-x}\text{Mn}_x\text{Te}$ quantum well, thus, provides interest on two levels. First, the static mean-field s - d contribution from the Mn ions produces a large Zeeman splitting:

$$Z_e(B) = \Delta - |g_e| \mu_B B, \quad (1)$$

where Δ is the Overhauser shift due to the Mn spin polarization and $-|g_e| \mu_B B$ is the normal Zeeman splitting of the conduction band (here $g_e \simeq -1.64$ for $\mu_B > 0$). This leads to a high spin polarization degree $\zeta = (n_\uparrow - n_\downarrow) / n_{2D}$ in the 2DEG.¹⁷ It makes it a suitable system to study features of spin-resolved Coulomb interaction.^{8,18} The above approach was followed in our previous work to study spin excitations of the spin-polarized 2DEG (SP2DEG).^{8,16,17,19} Propagative spin flip waves (SFW) of electrons were observed¹⁶ and their appearance was linked to the Coulomb interaction between electrons.¹⁷ On a second level, it provides evidence of the mixing between electrons and Mn spin modes in the frequency⁹ and time⁴ domains as predicted in Ref.⁷. Nevertheless, a connection between these manifestations needs to be made: in the first approach, s - d dynamical coupling with the Mn was neglected, while in the second, Coulomb interaction between electrons did not manifest experimentally and was not taken into account in theories of Ref.^{7,11}. There is, therefore, a lack of full understanding of the mixed spin-excitations where both Coulomb interactions between electrons and the s - d dynamical coupling with Mn spins interplay. Moreover, in the later studies,^{4,9} only the zone center collective electron-Mn modes were probed. From the Larmor's theorem,¹⁶ it is known that the spin system behaves as if the electrons

were not interacting through Coulomb. This explains why theories describing the electron-Mn modes, without the Coulomb interaction between carriers,⁷ agree well with the experimental data of Ref.⁹. Out of zone center, predictions of Ref.¹¹, found the out of phase mode (so-called stiff mode) to have a positive dispersion above the Stoner continuum. However, we have shown by angle-resolved Raman measurements that the collective electron spin mode (SFW mode), was below the spin-flip single-particle excitations (SF-SPE)⁸, together with a negative slope dispersion with the Raman transferred in plane momentum q .¹⁶ It is natural to make the correspondence between the stiff mode of Ref.¹¹ and the SFW mode of Refs.⁸ and¹⁶ (Stoner-like excitations are obviously the SF-SPE). Therefore, our experimental observations are in contradiction with the theory of Ref.¹¹.

In the following we will use the denomination "out of phase mode" or OPM to describe a mode which coincides with the stiff mode when the Coulomb interaction between carriers is neglected or to the SFW mode when the s - d dynamical coupling with Mn spins is neglected.

In this work, we want to resolve this contradiction, by first showing new experimental data that clearly shows the SF-SPE continuum and that the OPM propagates below it with a negative dispersion. Secondly, we will introduce a new propagator for the electron-Mn collective modes that includes the Coulomb interaction between spin-polarized carriers. Finally, we justify the experimental features by comparing the s - d exchange dynamical correction due to the coupling of the electron and Mn spin precession with the correction introduced by the Coulomb interaction between carriers. We will demonstrate that the ratio of these two corrections does not depend, at standard conditions, on the Mn concentration and that the Coulomb correction always dominates over the s - d dynamical shift except for very large electron densities.

II. SAMPLES AND EXPERIMENTAL SETUP

Our measurements were made in the back scattering geometry on a $\text{Cd}_{1-x}\text{Mn}_x\text{Te}$ single quantum well with electron densities $n_{2\text{D}}$ ranging from $2 \times 10^{11} \text{ cm}^{-2}$ to $4 \times 10^{11} \text{ cm}^{-2}$ and an effective Mn^{2+} concentration x_{Mn} ranging from 0.24% to 1%.¹⁸ The quantum wells were grown by molecular beam epitaxy on a GaAs substrate.²⁰ These quantum wells and their spin polarizations have been characterized in our previous publication.¹⁸ Here we will consider samples A and B of that reference. Both A and B have a density of $n_{2\text{D}} = 2.9 \times 10^{11} \text{ cm}^{-2}$ and different Mn concentrations, 0.46% and 0.75%, respectively. Measurements were taken with the samples immersed in superfluid helium at $\sim 1.5 \text{ K}$ inside a superconducting magnetic cryostat. The essential part of the cryostat is in the rod holding the sample, which allows for control in three directions, including rotation of the sample in the plane of the magnetic field for dispersions while the

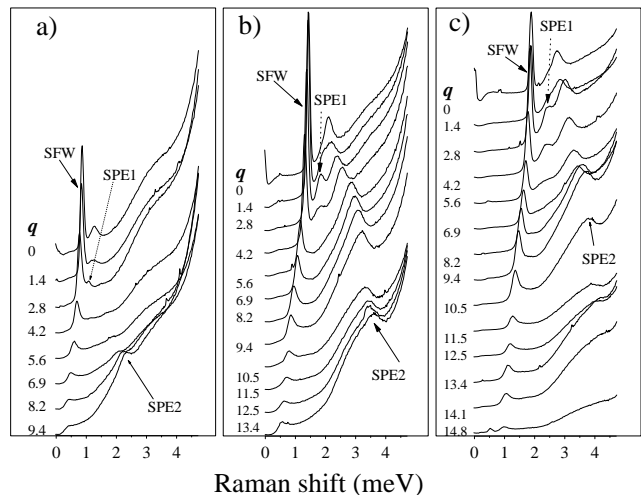


FIG. 1. Raman spectra of collective SFW and SF-SPE for magnetic fields: (a) $B = 0.6 \text{ T}$, (b) $B = 1.2 \text{ T}$ and (c) $B = 2.1 \text{ T}$ in sample A. Arrows indicate locations of SF-SPE, SPE1 and SPE2 as described in the text. The lines at 0 meV are remnants of the laser line.

collection/reflection mirror was kept fixed. This design aids in an easy study of the Raman scattering dispersions with an accuracy of 1 degree ($q = 0.3 \times 10^6 \mu\text{m}^{-1}$). To determine the in-plane wave vector q transferred in the plane of the quantum well, the angle of rotation θ is measured between the normal of incidence of the sample and the scattered light. q is obtained from the geometry of the set-up as $q \sim \frac{4\pi}{\lambda} \sin \theta$, where λ is the excitation wavelength.²¹ The holder was inserted in the core of a solenoid producing magnetic fields of up to 5 T in the plane of the quantum well. A tunable cw Ti-sapphire laser, pumped by an Ar^+ laser was used as light source. The laser power density was kept below 0.1 W/cm^2 and the linewidth was 0.3 cm^{-1} at a slit opening of $50 \mu\text{m}$. The energy of the laser was tuned to resonate close to the transition between the first conduction band and the second heavy hole band of the quantum well.

III. RESULTS AND DISCUSSION

In Fig. 1, we show typical Raman scattering spectra obtained on sample A for various Raman transferred momentum q obtained at different magnetic fields: (a) $B = 0.6 \text{ T}$, (b) $B = 1.2 \text{ T}$ and (c) $B = 2.1 \text{ T}$. In the figure, q varies from 0 to $\sim 15 \mu\text{m}^{-1}$. All spectra are dominated by a sharp-peaked line associated with the collective SFW as already demonstrated in Ref.¹⁶. We will show in the following that this mode is exactly the out of phase electron-Mn mode (the stiff mode of Ref.¹¹) of the DMS system. The SFW mode is narrow in width compared to the other excitations in the spectra and is found to be intense at all magnetic fields. As q is increased, the intensity and energy of the SFW decreases and eventually

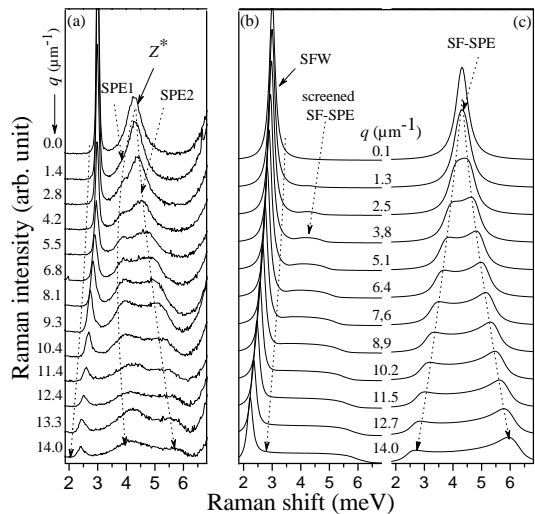


FIG. 2. Comparison between Raman spectra (a) at different q values taken on sample B with the corresponding calculated spectra (b) and (c). (b) is obtained from the collective response and (c) from the single particle response.

diminishes at a critical wave vector, q_c .¹⁷ The linewidth of the SFW broadens with increasing q , damping out due to interactions with the SF-SPE continuum.¹⁹

At high energies, features of the SF-SPE are observed in the spectra of Fig. 1. These features emerge as the magnetic field is increased, showing a fan-shaped like behavior at large q values leading to a continuum. This continuum corresponds to the joint density of state of electron-hole pairs in the Fermi sea which has a characteristic double-peak structure.¹⁷ In the following, we have labeled the maxima positions of the SF-SPE continuum as SPE1 and SPE2. In the long wavelength limit, SPE1 and SPE2 peaks are close to $Z^* \pm \hbar v_{F\uparrow} q$ where $v_{F\uparrow}$ is the Fermi velocity of the minority spin subband and Z^* is the renormalized Zeeman energy.⁸ SPE1 and SPE2 are degenerate at $q = 0$ forming a single peaked structure positioned at Z^* .⁸ At small wavevectors, a clear distinction between SPE1 and SPE2 is difficult as these features overlap. SPE1 shifts to low energies, decreasing in intensity and eventually vanishing as q is increased. SPE2 on the other hand, increases both in intensity and energy when increasing q . The dip between SPE1 and SPE2 is due to the occupancy of the upper spin subband.

In Fig. 2, we compare the Raman scattering spectra taken on sample B ($x_{Mn} = 0.75\%$ and $n_{2D} = 2.9 \times 10^{11} \text{ cm}^{-2}$) for various q with calculated spectra for the same conditions obtained from the collective response and the single particle response of Ref.¹⁷. The experimental spectra are neither given by the collective response, nor the single-particle one, but by a mixing of both responses. This is a consequence of the optical resonance with the incoming Raman photon.²²

We now plot in Fig. 3 the dispersions of the SFW and features of the SF-SPE extracted from Fig. 1 and compare with calculations. The spin polarizations in Fig.3(a)

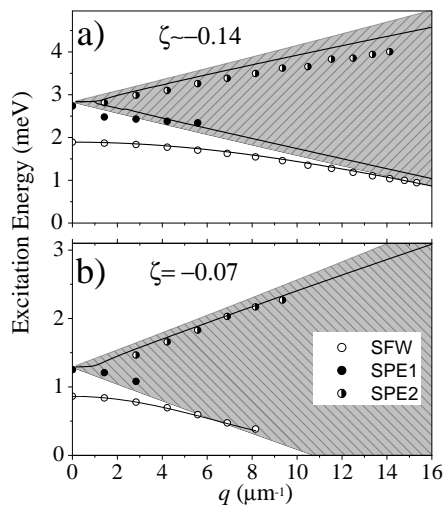


FIG. 3. Experimental dispersions of the SFW mode and features of the SF-SPE continuum extracted from Fig. 1(a) and (c). These, respectively, correspond to spin polarization values $\zeta = -0.14$ and $\zeta = -0.07$. Experimental data are compared with calculations: the dashed domain is the SF-SPE continuum, edges of the domain are given for $T = 0$ K. The lines inside the domain (when available) are the peaks of the single particle response [see Fig. 2(c)] calculated at $T = 2$ K. The line below the continuum is the OPM dispersion.

and 3(b) are respectively $\zeta = -0.14$ and $\zeta = -0.07$. In the spectra of Fig. 1 and the dispersions in Fig. 3, our data show clearly that the SFW mode propagates below the SF-SPE continuum with a negative slope dispersion at energies that are in exact agreement with the calculated OPM energy. Evidence is given that this experimental mode is the OPM (or stiff mode of Ref.¹¹). Consequently, our observations are in contradiction to this theory which predicted that the dynamical s - d exchange interaction between the Mn ions and the electrons shifts the OPM above the SF-SPE continuum with a positive dispersion. To resolve this contradiction, we have introduced the Coulomb interaction between carriers to calculate the coupled electron-Mn response. Details of the calculations are given in Ref.²³.

The mixed response function is calculated adiabatically and leads to the following electron spin susceptibility:

$$\left\langle \left\langle \hat{S}_{+, \mathbf{q}}; \hat{S}_{-, -\mathbf{q}} \right\rangle \right\rangle_{\omega} = \frac{(\hbar\omega - Z_{Mn}) \chi_{+}(\mathbf{q}, \omega)}{\hbar\omega - Z_{Mn} - K \Delta \frac{2\pi\hbar^2}{m^* Z^*} \chi_{+}(\mathbf{q}, \omega)} \quad (2)$$

where $\left\langle \left\langle \hat{S}_{+, \mathbf{q}}; \hat{S}_{-, -\mathbf{q}} \right\rangle \right\rangle_{\omega}$ is the linear response of the transverse electron spin fluctuation observable $\hat{S}_{+, \mathbf{q}}$ to the perturbation $g_e \mu_B b_{+, \mathbf{q}, \omega}$ created by a transverse magnetic field of temporal and spatial Fourier components, respectively, given by ω and \mathbf{q} .^{3,10} Coupled electron-Mn modes appear as poles of $\left\langle \left\langle \hat{S}_{+, \mathbf{q}}; \hat{S}_{-, -\mathbf{q}} \right\rangle \right\rangle_{\omega}$. In

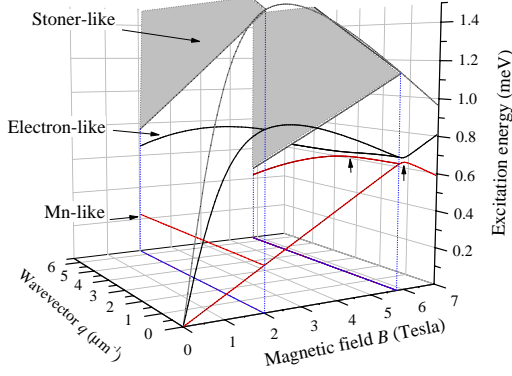


FIG. 4. (Color online) Electron-Mn modes as a function of both the magnetic field B and wavevector q . In the plane $q = 0$, the two lower curves are the solutions $\hbar\omega_{q=0}^{\pm}$ of Eq.(3). The OPM is the higher energy solution. The upper curve is the SF-SPE (Stoner-like excitations) degenerate to Z^* . Out of the resonant field ($B_R = 5.9\text{T}$) where the modes anti-cross, the branches have electron or Mn character. At the resonant field (indicated by a vertical arrow), the avoided gap is about $25 \mu\text{eV}$. In addition, dispersions $\hbar\omega_q^{\pm}$ obtained from Eq.(2) have been plotted for $B = 2 \text{ T}$ and $B = 5.5 \text{ T}$. For $B = 2 \text{ T}$ the electron or Mn characters of the mode do not change. However, for $B = 5.5 \text{ T}$ the modes anticross and an avoided gap appears at a finite q_R (indicated by the vertical arrow). Modes exchange their slope dispersions and characters when q varies across q_R . Calculations were done for $x_{\text{Mn}} = 0.24\%$, $T = 2 \text{ K}$, $n_{2\text{D}} = 3.13 \times 10^{11} \text{ cm}^{-2}$ and a square quantum well of width $w = 15 \text{ nm}$.

Eq.(2) $Z_{\text{Mn}} = g_{\text{Mn}}\mu_B B + K$ is the Mn spin precession energy in the presence of the 2DEG equilibrium spin polarization, g_{Mn} is the manganese g factor; μ_B is the Bohr magneton; m^* is the electron effective mass; $\chi_+(\mathbf{q}, \omega)$ is the SP2DEG spin susceptibility;¹⁷ $\Delta = \alpha\gamma x_{\text{Mn}} N_0 \left\langle \hat{S}_z^{Mn} \right\rangle (B, T)$ and $K = \frac{1}{2} \frac{\alpha\gamma}{w} n_{2\text{D}} |\zeta|$ are the Overhauser and Knight shifts, respectively. $N_0\alpha = 220 \text{ meV}$ ²⁴ is the s - d exchange integral and $\left\langle \hat{S}_z^{Mn} \right\rangle (B, T)$ is the thermal average spin of a single Mn atom. γ is the probability of finding an electron in the quantum well. Typical orders of magnitude in our samples of Δ and K are $\sim 10^{-3}$ and $\sim 10^{-6} \text{ eV}$, respectively. Interpretation of the poles is as follows. In the frame of the Mn ions, the Mn precession frequency is determined by the Zeeman energy of the Mn ($g_{\text{Mn}}\mu_B B$), the static mean-field s - d contribution from electrons (K), and the third term is the "dynamical" Knight shift that originates from the electron precession itself responding (through the $\chi_+(\mathbf{q}, \omega)$ response) to the Mn magnetic field (proportional to Δ). At $q = 0$, $\chi_+(\mathbf{q} = 0, \omega) = -n_{2\text{D}}\zeta / (\hbar\omega - Z_e)$, collective

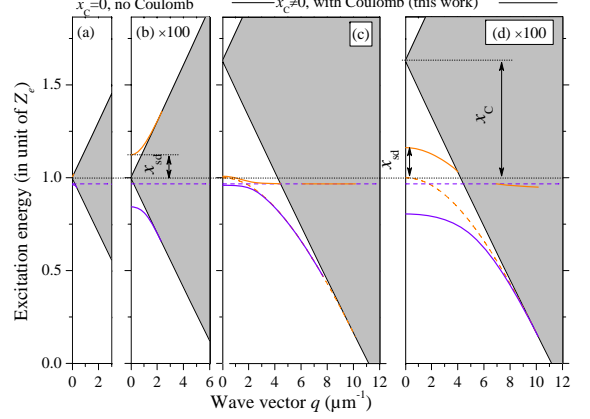


FIG. 5. (Color online) Illustration of the Coulomb and s - d dynamical shift on the electron-Mn modes dispersions. Dispersions were calculated for $B = 5.8 \text{ T}$ and the same sample parameters as in Fig.4. In (a) and (b), the Coulomb interaction between electrons is suppressed, only the s - d dynamical shift applies as in Eq.(20) of Ref.¹¹. The dashed line is the uncoupled Mn mode energy (Z_{Mn}). In (c) and (d), the Coulomb interaction between electrons is included as in Eq.(2) of this work. Dashed lines are the uncoupled electron mode ($\hbar\omega_q^{\text{SFW}}$) and Mn mode (Z_{Mn}). At $q = 0$ the SF-SPE energy is shifted to Z^* . In (b) and (d) the s - d dynamical coupling has been artificially magnified by a factor of 100.

modes of Eq.(2) develop two modes:

$$\hbar\omega_{q=0}^{\pm} = \frac{1}{2} \left(Z_{\text{Mn}} + Z_e \pm \sqrt{(Z_{\text{Mn}} - Z_e)^2 + 4K\Delta} \right), \quad (3)$$

where $Z_{\text{Mn}} = g_{\text{Mn}}\mu_B B + K$. They open an avoided gap at a specific magnetic field B_R when $Z_{\text{Mn}} - Z_e = 0$, as illustrated in Fig.4 where $B_R = 5.9 \text{ T}$ for $x_{\text{Mn}} = 0.24$. The upper (resp. lower) energy branch is the OPM (resp. in phase). For $B < B_R$, the OPM (resp. in phase) has an "Electron like" character (resp. "Mn-like"), because it is mainly dominated by the electron (resp. Mn) spin precession. In resonance ($B = B_R$) modes have a complete mixed character. These zone center modes were observed in Ref.⁹ and Ref.⁴. The resonance field depends mainly on the Mn concentration and for the experimental situation of Fig.3, it is about 10.7 T . Figure 3 compares the dispersion of the OPM $\hbar\omega_q^+$, calculated using Eq.(2) and the parameters of sample A, with the experimental one. Undoubtedly, the agreement with the data is excellent without any fitting procedure. The dispersion of the SFW mode $\hbar\omega_q^{\text{SFW}}$ defined as the unique pole of $\chi_+(\mathbf{q}, \omega)$ is also plotted. It appears that the introduction of the s - d dynamical coupling shifts $\hbar\omega_q^+$ negligibly from the pure electron mode $\hbar\omega_q^{\text{SFW}}$ for that situation. However, the inclusion of the Coulomb interaction in Eq.(2) positions the OPM below the SF-SPE continuum with a negative dispersion, contrary to what was found in Ref.¹¹.

Illustration of this phenomenon is provided in Fig.5. In

Fig. 5(a) and (b) the electron-Mn modes dispersion were calculated using the denominator of Eq.(2) by replacing the SP2DEG spin susceptibility with the non-interacting equivalent, which is single particle response [see Ref.¹⁷]. Such a calculation is equivalent to the approach of Ref.¹¹. Thus, for no Coulomb interaction between electrons, the pure electron modes are the SF-SPE (poles of the single-particle response) degenerate to Z_e at $q = 0$. Inclusion of the s - d dynamical coupling with the Mn introduces a collective OPM propagating above the SF-SPE continuum (upper curve in Fig. 5(a) and (b)). The relative "blue-shift" is labeled x_{sd} . In presence of Coulomb interaction between carriers, however, a collective electron mode (SFW) appears and propagates below the SF-SPE continuum with a negative dispersion given by $\hbar\omega_q^{SFW}$. The SF-SPE zone center energy is "blue shifted" from Z_e to Z^* by Coulomb-exchange. The relative "red-shift" of the SFW mode with the SF-SPE is labeled x_C . Inclusion of the s - d dynamical coupling with Mn introduces a new shift which determines the final energy of the OPM.

Thus, we have separated two effects. First, Coulomb introduces a shift between the collective electron mode and the SF-SPE energies with a relative quantity quantifiable by $x_C = (Z^* - Z_e)/Z_e$. Second, the s - d dynamical coupling with the Mn shifts this mode to $\hbar\omega_q^+$ with a relative shift quantifiable as $x_{sd} = (\hbar\omega_{q=0}^+ - Z_e)/Z_e$. Clearly, in the situation of Fig.3: $x_C \gg x_{sd}$.

We may ask if conditions can be found such that $x_{sd} > x_C$? If so, the OPM would propagate above the SF-SPE continuum with a positive slope dispersion. We should distinguish two situations. For $B < B_R$:

$$x_{sd} \simeq \frac{K\Delta}{Z_e^2} \approx \frac{K}{Z_e} = \frac{Z^* \alpha \gamma m^*}{Z_e 4\pi\hbar^2} \frac{1}{w}. \quad (4)$$

In resonance, however, ($B = B_R$),

$$x_{sd}(r) = \frac{\sqrt{K\Delta}}{Z_e} \simeq \sqrt{x_{sd}}.$$

In Figure 6, we compare x_{sd} calculated out of resonance and $x_{sd}(r)$ calculated in resonance with x_C for quantum well widths, $w = 50 \text{ \AA}$ and $w = 150 \text{ \AA}$. Both x_{sd} and $x_{sd}(r)$ are calculated as a function of the electron density, plotted in terms of r_s . As seen in Fig. 6, the dynamical shift $x_{sd}(r)$ overcomes the Coulomb effect at a sufficiently low electron density corresponding to $r_s = 0.2$ and 0.08 . The out of resonance dynamical shift x_{sd} overcomes the Coulomb effect at much lower densities.

We now simulate a situation in which a prediction with $\hbar\omega_q^+$ propagating above the SF-SPE is possible. We have assumed the material parameters of Fig. 6, that is, when the dynamical shift dominates the Coulomb shift. We show such calculated dispersions of mixed spin modes in Fig. 7 for $r_s = 0.1$. Indeed, the electron modes appear above the SF-SPE continuum. However, to obtain

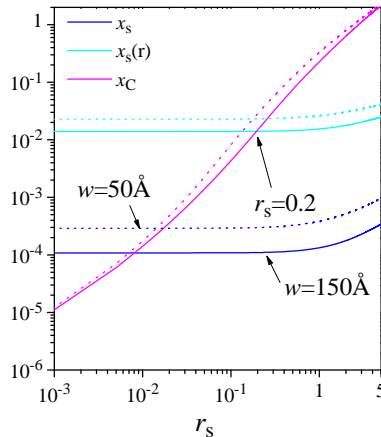


FIG. 6. (Color online) Comparison of the dynamical shift x_{sd} calculated out or in resonance ($x_{sd}(r)$) with the Coulomb shift x_C . Both are calculated as a function of the electron density for a fixed quantum well width, $w = 50 \text{ \AA}$ (dotted lines) and $w = 150 \text{ \AA}$ (full lines). The dynamical shift $x_{sd}(r)$ overcomes x_C for a sufficiently low electron density (respectively $r_s = 0.2$ and 0.08). The out of resonance dynamical shift x_{sd} overcomes the Coulomb effect at much lower densities.

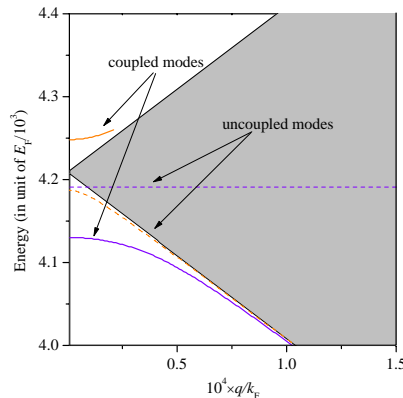


FIG. 7. (Color online) Dispersions of mixed spin modes calculated using the parameters of Fig.6(a) for $r_s = 0.1$. The electron modes appear above the SF-SPE continuum. To get the effect, the Mn concentration is raised to $x_{Mn} = 10\%$ in order to get $\zeta = 0.2\%$. The external magnetic field is tuned to $B_R = 130 \text{ T}$. Here $w = 150 \text{ \AA}$ and $T = 2 \text{ K}$.

such an effect, a significant spin polarization of $\zeta = 0.2\%$ must be reached by raising the Mn ion concentration to $x_{Mn} = 10\%$. This means that an external magnetic field needs to be tuned to a resonant field of $B_R = 130 \text{ T}$, an experimental challenge! We note here that the small blue shift introduced to the SFW energy by the dynamical coupling x_{sd} , explains the near excellent agreement between our previous model and experiment. Since

the Coulomb effect dominates in our quantum well, the mixed modes evolve essentially as an electron wave.

IV. CONCLUSIONS

We have probed dispersions of spin flip waves and spin flip single particle excitations in a spin polarized electron gas in a $\text{Cd}_{1-x}\text{Mn}_x\text{Te}$ quantum well using angle-resolved Raman scattering. Our key result is that the SFW dispersion lies below the SF-SPE continuum, contrary to predictions made by the theory of spin waves in diluted magnetic systems. Analysis of our measurements with a model accounting for the Coulomb interaction between carriers and the dynamical response of Mn ions and the electron spin subsystem in the spin wave propagator of the theory agrees well with our experimental

results. We have found that the Coulomb contribution dominates over the dynamical response. We have investigated a regime in which the dynamical coupling overcomes the Coulomb effect and find this to occur at an extremely large external magnetic field and for a high Mn ion concentration.

ACKNOWLEDGMENTS

The authors would like to thank Jules Silembo, Michel Menant and Silbe Majrab for machining parts of the magnetic cryostat and electronics used in the experiments. Special thanks to Dimitri Roditchev for experimental help. This work was partially supported by the EP-SRC and the CNRS. Additional financial support was provided by the grant ANR GOSPININFO.

-
- ¹ I. Garate and A. MacDonald, Phys. Rev. B **79**, 064404 (2009).
- ² M. D. Kapetanakis and I. E. Perakis, Phys. Rev. Lett. **101**, 097201 (2008).
- ³ J. Qi, Y. Xu, A. Steigerwald, X. Liu, J. K. Furdyna, I. E. Perakis, and N. H. Tolk, Phys. Rev. B **79**, 085304 (2009).
- ⁴ M. Vladimirova, S. Cronenberger, P. Barate, D. Scalbert, F. J. Teran, and v A. P. Dmitrie, Phys. Rev. B **78**, 081305(R) (2008).
- ⁵ T. Dietl, H. Ohno, F. Matsukura, J. Cibert, and D. Ferrand, Science **287**, 1019 (2000).
- ⁶ J. König, H.-H. Lin, and A. H. MacDonald, Phys. Rev. Lett. **84**, 5628 (2000).
- ⁷ J. König and A. H. MacDonald, Phys. Rev. Lett. **91**, 077202 (2003).
- ⁸ F. Perez, C. Aku-Leh, D. Richards, D. W. B. Jusserand, L. C. Smith, and G. Karczewski, Phys. Rev. Lett. **99**, 026403 (2007).
- ⁹ F. J. Teran, M. Potemski, D. K. Maude, D. Plantier, A. K. Hassan, A. Sachrajda, Z. Wilamowski, J. Jaroszynski, T. Wojtowicz, and G. Karczewski, Phys. Rev. Lett. **91**, 077201 (2003).
- ¹⁰ A. Mauger and D. L. Mills, Phys. Rev. B **28**, 6553 (1983).
- ¹¹ D. Frustaglia, J. König, and A. H. MacDonald, Phys. Rev. B **70**, 45205 (2004).
- ¹² Y. Hashimoto, S. Kobayashi, and H. Munekata, Phys. Rev. Lett. **100**, 067202 (2008).
- ¹³ D. M. Wang, Y. H. Ren, X. Liu, J. K. Furdyna, M. Grimsditch, and R. Merlin, Phys. Rev. B **75**, 233308 (2007).
- ¹⁴ K. Khazen, H. J. von Bardeleben, J. L. Cantin, L. Thevenard, L. Largeau, O. Mauguin, and A. Lemaître, Phys. Rev. B **77**, 165204 (2008).
- ¹⁵ H. Boukari, F. Perez, D. Ferrand, P. Kossacki, B. Jusserand, and J. Cibert, Phys. Rev. B. **73**, 115320 (2006).
- ¹⁶ B. Jusserand, F. Perez, D. R. Richards, G. Karczewski, T. Wojtowicz, C. Testelin, D. Wolverson, and J. J. Davies, Phys. Rev. Lett. **91**, 086802 (2003).
- ¹⁷ F. Perez, Phys. Rev. B. **79**, 045306 (2009).
- ¹⁸ C. Aku-Leh, F. Perez, B. Jusserand, D. Richards, W. Pacuski, P. Kossacki, M. Menant, and G. Karczewski, Phys. Rev. B **76**, 155416 (2007).
- ¹⁹ J. Gómez, F. Perez, E. M. Hankiewicz, B. Jusserand, G. Karczewski, and T. Wojtowicz, Phys. Rev. B **81**, 100403(R) (2010).
- ²⁰ G. Karczewski, J. Jaroszynski, A. Barcz, M. Kutrowski, T. Wojtowicz, and J. Kossut, J. Cryst. Growth **184/185**, 814 (1998).
- ²¹ There is an additional factor of $\cos \alpha/2$, where α is the angle between the scattered and incident light. The normal of incidence is taken as the zero. α is typically small (≤ 2 degrees). Therefore $\cos \alpha \simeq 1$.
- ²² S. DasSarma and D.-W. Wang, Phys. Rev. Lett. **83**, 816 (1999).
- ²³ F. Perez and et al., To be published.
- ²⁴ J. A. Gaj, R. Planel, and G. fishman, Solid State Comm **29**, 435 (1979).